Available online at www.sciencedirect.com

SCIENCE DIRECT

Virology 349 (2006) 409–421

VIROLOGY

www.elsevier.com/locate/yviro

Differential distribution of non-structural proteins of foot-and-mouth disease virus in BHK-21 cells

Mercedes García-Briones [a,b], María F. Rosas [a], Mónica González-Magaldi [a], Miguel A. Martín-Acebes [a], Francisco Sobrino [a,b,*], Rosario Armas-Portela [a,c,*]

[a] *Centro de Biología Molecular "Severo Ochoa" (CSIC-UAM), Spain*
[b] *Centro de Investigación en Sanidad Animal, INIA, Valdeolmos, 28130 Madrid, Spain*
[c] *Departamento de Biología, Facultad de Ciencias, Universidad Autónoma de Madrid, Cantoblanco, 28049 Madrid, Spain*

Received 14 November 2005; returned to author for revision 13 December 2005; accepted 28 February 2006
Available online 19 April 2006

Abstract

Differences in the kinetics of expression and cell distribution among FMDV non-structural proteins (NSPs) have been observed in BHK-21-infected cells. $3D^{pol}$ was the first protein detected by immunofluorescence (1.5 h p.i.), showing a perinuclear distribution. At 2–2.5 h p.i., 2B, 2C, 3B and 3C were detected, mostly exhibiting a punctuated, scattered pattern, while 3A and $3D^{pol}$ appeared concentrated at one side of the nucleus. This distribution was exhibited by all the NSPs from 3 h p.i., being 2C and, to a lesser extent, precursors 2BC and 3ABBB, the only proteins detected by Western blotting at that infection time. From 4 h p.i., all mature NSPs as well as precursors 2BC, 3ABBB, 3ABB, 3AB and $3CD^{pol}$ were detected by this technique. In spite of their similar immunofluorescence patterns, 2C and 3A co-localized partially by confocal microscopy at 3.5 h p.i., and 3A, but not 2C, co-localized with the ER marker calreticulin, suggesting differences in the distribution of these proteins and/or their precursors as infection proceeded. Transient expression of 2C and 3AB resulted in punctuated fluorescence patterns similar to those found in early infected cells, while 3A showed a more diffuse distribution. A shift towards a fibrous pattern was noticed for 3ABB, while a major change was observed in cells expressing 3ABBB, which displayed a perinuclear fibrous distribution. Interestingly, when co-expressed with $3D^{pol}$, the pattern observed for 3ABBB fluorescence was altered, resembling that exhibited by cells transfected with 3AB. Transient expression of $3D^{pol}$ showed a homogeneous cell distribution that included, as determined by confocal microscopy, the nucleus. This was confirmed by the detection of $3D^{pol}$ in nuclear fractions of transfected cells. $3D^{pol}$ and its precursor $3CD^{pol}$ were also detected in nuclear fractions of infected cells, suggesting that these proteins can directly interact with the nucleus during FMDV infection.

Keywords: FMDV; Non-structural proteins; Subcellular distribution; Infection; Transient expression

Introduction

Foot-and-mouth disease virus (FMDV), an aphthovirus that belongs to the Picornaviridae family, is the causative agent of one of the most economically damaging animal diseases (Bachrach, 1977; Domingo et al., 1990; Pereira, 1981; Sobrino et al., 2001). FMD affects domestic and wild artiodactyls, mainly cattle, swine, goats and sheep, producing a typical vesicular disease (Burrows et al., 1981). FMDV genome consists of a positive-sense RNA molecule of approximately 8500 nucleotides that encodes a unique polyprotein, which is processed in infected cells to yield different polypeptide precursors and the mature viral proteins (Belsham, 2005). Replication and translation of FMDV RNA occur in the cytoplasm (Arlinghaus and Polatnick, 1969) and for certain Picornaviruses its capacity to replicate in enucleated infected cells has been reported (Follett et al., 1975). FMDV polyprotein synthesis can initiate at two in frame AUG codons (Beck et al., 1983) following ribosome recognition of the adjacent internal ribosome entry site (IRES) region (Belsham, 2004; Martinez-Salas, 1999). The open reading frame of FMDV sequentially

* Corresponding authors. Mailing address: CBMSO, Cantoblanco 28049, Madrid, Spain. Fax: +34 91 4978087.
E-mail addresses: fsobrino@cbm.uam.es (F. Sobrino), rarmas@cbm.uam.es (R. Armas-Portela).

0042-6822/$ - see front matter © 2006 Elsevier Inc. All rights reserved.
doi:10.1016/j.virol.2006.02.042

encodes a viral protease (L), the capsid or structural proteins, and a total of nine additional mature, non-structural proteins (NSPs). Enzymatic activities have been identified for proteases L, 2A and 3C, the latter responsible for most of the proteolytic processing of the viral polyprotein (Ryan et al., 2004), and for $3D^{pol}$, the virus-encoded RNA-dependent RNA polymerase (Newman et al., 1979).

The analysis of interactions of NSPs with cell structures in the context of FMDV infection is limited by the detection sensitivity of the specific antibodies available, as well as by the complexity of the virus–cell interactions occurred during viral cycle. Transient expression has provided a good tool to achieve information on the functional role of these proteins and has been extensively used to study Picornavirus cell interactions (Cho et al., 1994; Egger et al., 2000; Moffat et al., 2005; O'Donnell et al., 2001; Sandoval and Carrasco, 1997; Towner et al., 1996).

In other Picornaviruses, such as poliovirus, each of the equivalent NSPs and most of their precursors are known to be involved in multiple functions needed for RNA replication, particle formation and viral pathogenesis (Andino et al., 1999; Choe et al., 2005; Porter, 1993; Whitton et al., 2005). Thus, rearrangements of the host cell membranes to generate vesicular structures associated to genomic RNA replication have been reported (Bienz et al., 1987; Gazina et al., 2002; Gosert et al., 2000) and proteins 2B, 2BC, 2C and 3A are involved in these interactions (Aldabe and Carrasco, 1995; Cho et al., 1994; Towner et al., 1996).

FMDV proteins 2B, 2C and 3A are predicted to contain hydrophobic domains (Forss et al., 1984) and have been recently found associated to crude membrane extracts in infected cultured cells (Moffat et al., 2005). The genomic organization of the region encoding FMDV proteins 3A and 3B is unique among the Picornaviridae family in that 3A extends its carboxy-terminus in at least 60 amino acid residues in length. Mutations in this protein are associated with modifications of the virus host range (Beard and Mason, 2000; Nunez et al., 2001). In addition, three non-identical copies of 3B are encoded and expressed in susceptible cells, and deletions of redundant copies lead to a decrease in replication efficiency in cell culture (Falk et al., 1992) and attenuation in pigs (Pacheco et al., 2003). It has been recently shown that 3D can uridylylate in vitro the three copies of 3B (Nayak et al., 2005), an initial step required to initiate replication of positive-sense genomic RNA in Picornavirus (reviewed in Andino et al. (1999)). In poliovirus, 3AB has a non-specific RNA-binding activity and associates with the cloverleaf structure in the 5′ end of viral RNA and with precursor 3CD to form a ribonucleoprotein complex required for poliovirus RNA synthesis (Hope et al., 1997; Lama et al., 1994; Xiang et al., 1995, 1998).

Specific membrane rearrangements induced by FMDV in infected cells have been recently reported, such as its insensitivity to brefeldin A (O'Donnell et al., 2001). This drug blocks the function of ADP ribosilation factor 1 (ARF1) that is necessary for COPI-coated vesicle formation and disrupts the Golgi complex (Jackson and Casanova, 2000; Klausner et al., 1992). A collapse of cell organelles at one side of the cells (Monaghan et al., 2004) and the lack of ER or Golgi markers in the infection-recruited membranes (Knox et al., 2005) have also been reported as differential effects of FMDV infection. In poliovirus and coxackievirus, 3A, but not 3AB, is responsible of the inhibition of the anterograde traffic between the ER and the Golgi (Doedens et al., 1997), resulting in a reduction of the secretion of proteins such as MHC class I molecules (Choe et al., 2005), which is observed during Picornavirus infection (Deitz et al., 2000; Sanz-Parra et al., 1998). This mechanism could contribute to the evasion of the host immune system. Recent results with FMDV indicate that transient expression of 2BC, but not of 3A, inhibits host protein secretion in Vero cells (Moffat et al., 2005).

Host membrane recruitment to form the replication complex in Picornaviruses can involve components from different membrane compartments (Schlegel et al., 1996; Suhy et al., 2000). Early-induced vesicles by poliovirus infection are mostly recruited from ER-derived membranes (Bienz et al., 1987), while markers from other organelles, such as the Golgi and lysosomes, can be found in vesicles formed at later stages of infection (Bolten et al., 1998).

Despite of the information available, much remains to be understood on the detailed intracellular distribution of the FMDV NSPs precursors and mature proteins during the infection cycle and its relationship with the mechanism contributing to FMDV replication and pathogenesis. As a first step to address the functional role of the FMDV NSPs, we have analyzed the kinetics of detection and intracellular location of viral proteins 2B, 2C, 3A, 3B, 3C and $3D^{pol}$, and their precursors, in BHK-21 cells. This cell line has been widely used for basic FMDV studies, as well as for diagnostic assays and production of vaccine antigens (Barteling, 2004; Brown, 1998). This study has revealed differences in their early kinetics of expression and in the immunofluorescence patterns that NSPs display in infected cells. In addition, transient expression of single FMDV NSP products has provided evidences of distinct interactions of proteins $3D^{pol}$, 3A, 3AB, 3ABB and 3ABBB with host cell components.

Results

Expression and subcellular distribution of NSPs in FMDV-infected cells

The kinetics of NSPs expression in BHK-21-infected cells was first analyzed by Western blotting of cell extracts collected at different times upon infection, using specific antibodies to 2C, 3A, 3B, 3C and $3D^{pol}$ proteins. Detection of 2B expression was not possible as the serum available for this protein did not work in this assay. An MAb specific to capsid protein VP1 was also included in this analysis (Fig. 1A). The earliest protein detected (2.5 h p.i.) was 2C. A band corresponding to VP1 and faint bands corresponding to precursors P1, 2BC and 3ABBB (the latter with the anti 3B antibody) were observed at 3 h p.i. All the mature proteins analyzed were clearly observed at 4 h p.i., as well as precursors 2BC, 3ABBB, 3ABB, 3AB, and P1. Due to its similar size, 3A and 3AB co-migrated in the gel revealed with the antibody to 3A shown in Fig. 1A; however, the two proteins

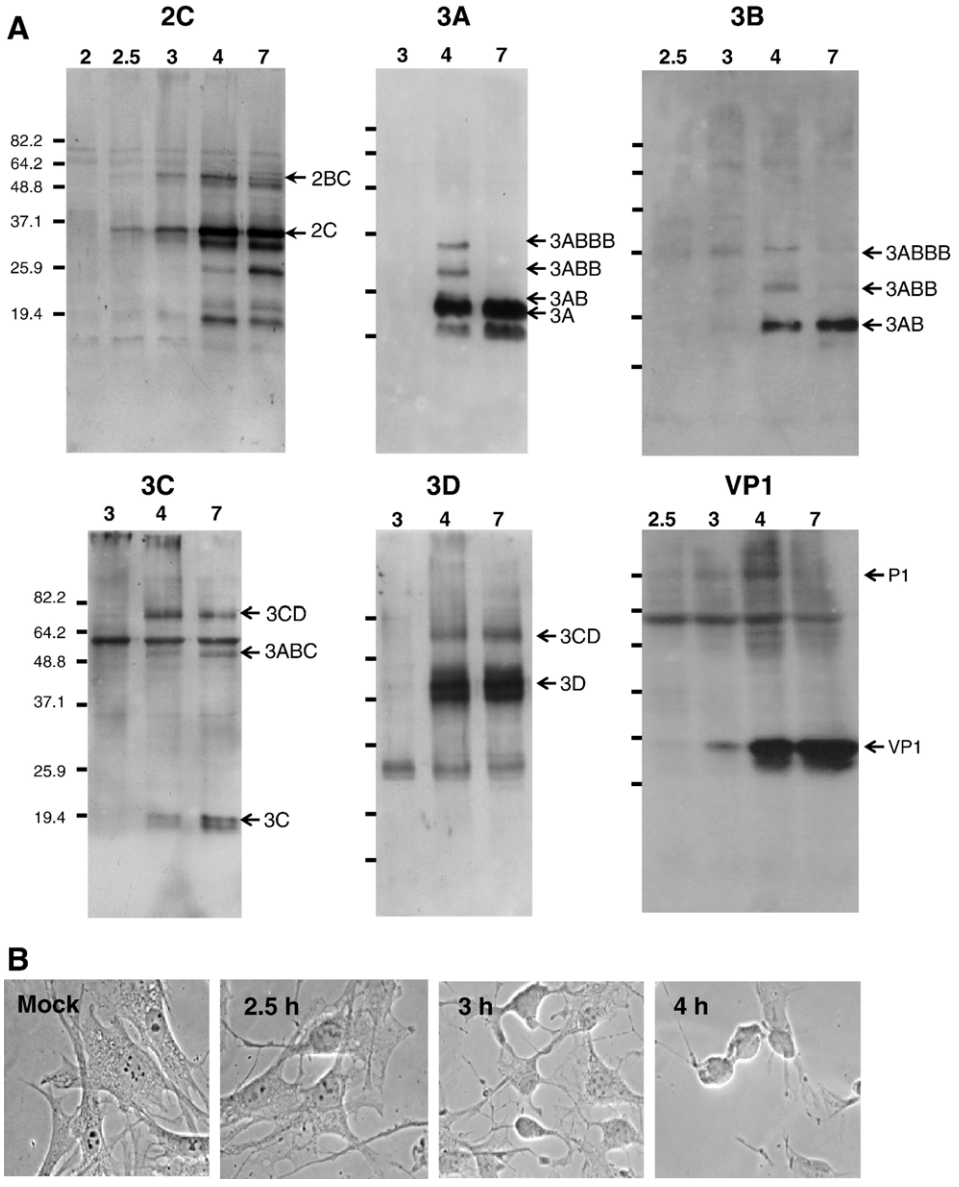

Fig. 1. Kinetics of FMDV infection in BHK-21 cells. (A) Western blot assays of cells collected at different times p.i. using antibodies to each of the viral proteins indicated. The migration of the markers and their molecular weight are indicated. Arrows point to the protein bands corresponding to the different FMDV proteins and their major precursors, according to Belsham (2004) and Toja et al. (1999). The predicted sizes (in kDa) of the FMDV proteins identified were: 52.7 (2BC), 35.8 (2C), 17.4 (3A), 20.1 (3AB), 22.7 (3ABB), 25.3 (3ABBB), 3ABC (47.4) 22.1 (3C), 75.7 ($3CD^{pol}$), 52.7 ($3D^{pol}$), 81 (P1), 22.9 (VP1). The mobility observed for 3A, 3AB, 3ABB and 3ABBB was slightly lower than that predicted, as also reported for other FMDV serotypes (O'Donnell et al., 2001). Doublets observed for 3D and VP1 could result from incomplete reduction of these proteins. The specific antibodies used are described in Materials and methods (MAb 1C8 and 2C2 were used for 2C and 3A detection, respectively). (B) Morphological alterations induced in infected cells at different times p.i., as determined by contrast-phase microscopy.

could be resolved using a higher polyacrylamide concentration (data not shown). By 7 h p.i., all mature proteins were detected as well as precursors 2BC, 3AB, 3ABC and 3CD and a protein band of a size corresponding to 3ABC was observed with the antibody to 3C. Antibodies to 2C and 3A also revealed the presence of protein bands of a size lower than expected at 4 and 7 h p.i. These products could result from proteolysis of these proteins and/or its precursors.

Accumulation of FMDV proteins correlated with the emergence of morphological signs of cytopathic effect in infected cells observed by contrast-phase microscopy. Progress of morphological alterations was not synchronic, and cells with different degrees of alteration could be observed during infection. In average, cells started loosing their characteristic morphology by 3 h p.i., turning by 4 h p.i. into rounded cells that became progressively detached from the plates (Fig. 1B).

A parallel analysis by immunofluorescence microscopy revealed differences in the temporal distribution of these proteins and their processing precursors in infected cells (Fig. 2). Specific $3D^{pol}$ immunostaining was detected, mostly showing a perinuclear distribution, as soon as 1.5 h p.i. From 2 h p.i., $3D^{pol}$ appeared concentrated at one side of the nucleus. Fluorescence of antibodies to VP1, 2B, 2C, 3A, 3B, 3C and their precursors was only observed from 2 to 2.5 h p.i. Immunostaining to 3A

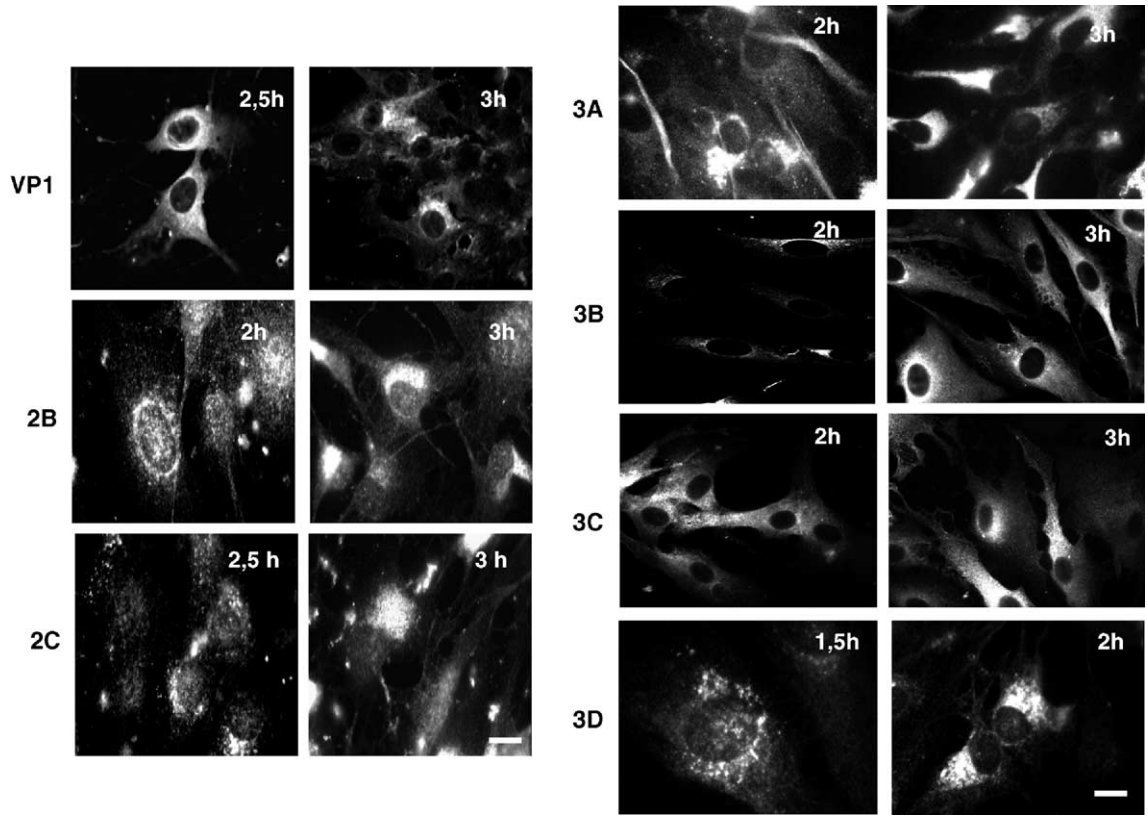

Fig. 2. Distribution of FMDV NSPs in BHK-21 cells at different times after infection. Infected cells were processed for immunofluorescence staining as described in Materials and methods. The following MAb and rabbit specific sera were used as primary antibodies: VP1 (SD6), DM21 (2B), E39 (2C), 2C2 (3A), 1F8 (3B), 2D2 (3C) and E56 (3D). Alexa Fluor 488 anti-rabbit and Alexa Fluor 594 anti-mouse antibodies were used as secondary antibodies to detect rabbit sera and MAbs, respectively. Scale bar, 10 μm.

showed a juxtanuclear distribution at 2 h p.i., similar to that of $3D^{pol}$ at this time of infection. Conversely, VP1, 2B, 2C and 3C mostly exhibited a punctuated and scattered pattern.

As infection proceeded (3 h p.i.), fluorescence to all the proteins analyzed accumulated in a juxtanuclear region that resembled that exhibited at earlier times (2 h p.i.) by $3D^{pol}$ and 3A (Fig. 2), probably reflecting their association to the replication complex. By 3 h p.i., a significant fraction of infected cells had already developed morphological alterations, as judged by contrast-phase microscopy (Fig. 1B).

In spite of their similar immunofluorescence patterns, differences in the distribution of 2C and 3A could be observed from 3.5 h p.i. by double labeling and confocal microscopy. Staining to antibodies E12 (3A) and 1C8 (2C) exhibited a similar bright pattern in most of the cells. However, the merge image revealed an incomplete co-localization of these proteins (Fig. 3A). This was confirmed by confocal image analyses using Metamorph co-localization menu, which rendered a correlation value of 0.60 ± 0.02. Interestingly, around 10% of infected cells mainly showed fluorescence to either 3A or 2C. In this case, lower correlation values (0.3) were obtained. These results suggest differences in the kinetics of accumulation and the intracellular location between these two proteins during the infection progress.

The involvement of 2C and 3A in interactions with cell membranes described for FMDV and other Picornaviruses led us to study a possible co-localization of these NSPs with ER or the Golgi markers. By using a rabbit antibody against calnexin, an ER marker, a reticular fluorescence pattern distributed throughout the cytoplasm was noticed, and no evidences of co-localization with proteins 3A (Fig. 3A) and 2C (data not shown) were observed by confocal microscopy of infected cells. Fluorescence to a different ER marker, calreticulin, appeared distributed with a more diffuse pattern and showed a partial co-localization (0.64 ± 11) with that of 3A, while no co-localization was observed with protein 2C (Fig. 3B). On the other hand, double immunofluorescence using MAb to p58 K protein (an anti-Golgi stacks marker) showed a partial co-localization with 3A and 2C after 3.5 h of BHK-21 infection (Fig. 3C). The thickness of the sections required to detect fluorescence of MAb CC92 to the *cis*-Golgi network protein gp74 impaired a confocal analysis of its co-localization with the anti-FMDV 3A and 2C antibodies in infected cells. However, an alteration of the distribution pattern of gp74 was noticed in infected cells (Fig. 3D), indicating a relocation of this *cis*-Golgi protein during infection.

Subcellular distribution of single NSPs transiently expressed in BHK-21 cells

As a complementary approach to study the role of FMDV NSPs in cell pathogenesis, we analyzed their distribution and

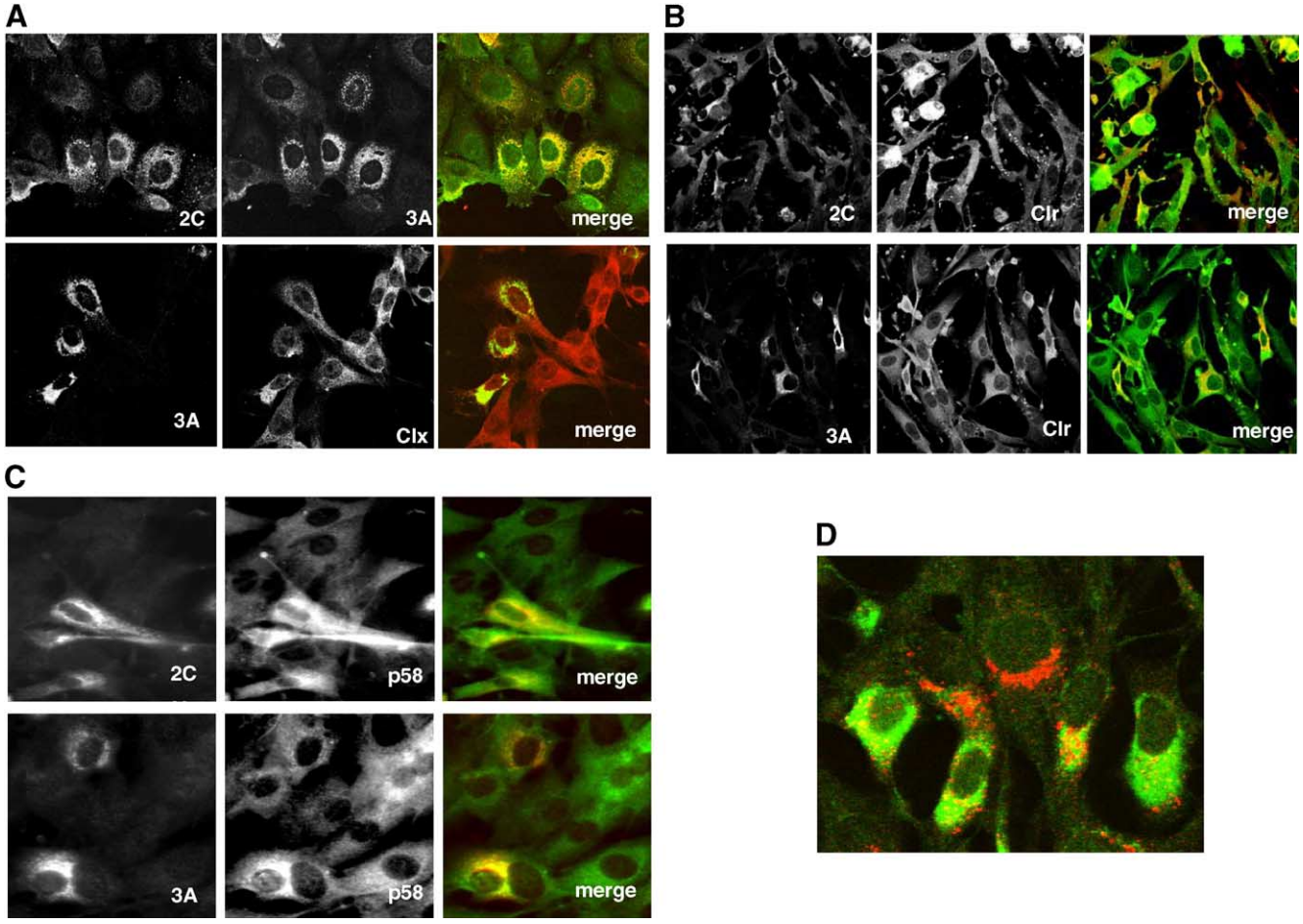

Fig. 3. Double immunofluorescence analysis of the distribution of 2C, 3A and ER or Golgi markers in BHK-21-infected cells. (A) Confocal images of partial co-localization of 2C and 3A revealed with MAb 1C8 and E12 rabbit serum (3A) (top) and of 3A and calnexin stained with MAb 2C2 and a rabbit anti-calnexin serum, respectively (clx, bottom). (B) Confocal images of co-localization of 2C and 3A and calreticulin (clr). MAbs 1C8 (2C) and 2C2 (3A) and a rabbit serum anti-calreticulin were used as primary antibodies. (C) Partial co-localization of 2C and 3A with Golgi stacks. Rabbit antisera E39 (2C) and E12 (3A) and MAb anti-p58 were used as primary antibodies. (D) Double immunofluorescence to 3A and the *cis*-Golgi network protein gp74 revealed with rabbit antiserum E12 and MAb CC92, respectively. The following secondary antibodies were used: A and C, Alexa 594 anti-rabbit (red) and Alexa 488 anti-mouse IgGs (green); B and D, Alexa 488 anti-rabbit (green) and Alexa 594 anti-mouse IgGs (red).

the cellular effects they produced when transiently expressed in BHK-21 cells from plasmid pRSV derivatives (see Materials and methods for details). Expression of 2B protein could not be detected at different times p.t. with plasmid pRSV-2B, neither by Western blotting nor by immunofluorescence. Transfection with pRSV-2C resulted in detectable levels of protein by Western blotting (data not shown), and cells exhibiting specific 2C fluorescence were observed at 24 and 48 h p.t. The rate of expressing cells was low (about 1%), as was the intensity of the fluorescence in positive cells, which showed a perinuclear distribution pattern (Fig. 4A). This pattern was similar to that observed for 2C at early times upon infection (Fig. 2). Cells positive to 2C showed an elongated morphology that impaired conclusive results in the analysis of the co-localization of 2C with PDI or the Golgi p58 protein.

About 10% of the cells transfected with pRSV-3A showed high levels of specific fluorescence at 24 h p.t., being these values lower at 48 h p.t. Expression of 3A was detected by Western blotting (Fig. 4B), and its fluorescence displayed a cytoplasmic diffuse pattern in most of the positive cells (Fig. 4A).

Since 3A precursors including one, two or the three non-identical copies of 3B proteins were found in FMDV-infected cells (see Fig. 1A), we analyzed the fluorescence pattern to 3A in cells transfected with pRSV-3AB, pRSV-3ABB or pRSV-3ABBB, whose expression levels, detected with an anti-3A MAb, were similar to that found in cells transfected with pRSV-3A (Fig. 4A). Expression of 3AB, a precursor found in infected cells at both early and late phases of infection (Fig. 1A), was distributed in a scattered punctuated fluorescence pattern (Fig. 4A), and a protein band of the expected size was observed by Western blotting (Fig. 4B). Double immunofluorescence experiments did not show co-localization with PDI or with Golgi p58, and no significant alterations in the distribution pattern of these cell proteins were observed in cells expressing 3A or 3AB (data not shown).

The fluorescence shown by cells expressing 3ABB appeared more compact, displayed a fibrous pattern and a protein band corresponding to this polypeptide was detected in cell extracts (Figs. 4A, B). Remarkably, expression of 3ABBB resulted in a different distribution that showed a fibrous and often perinuclear

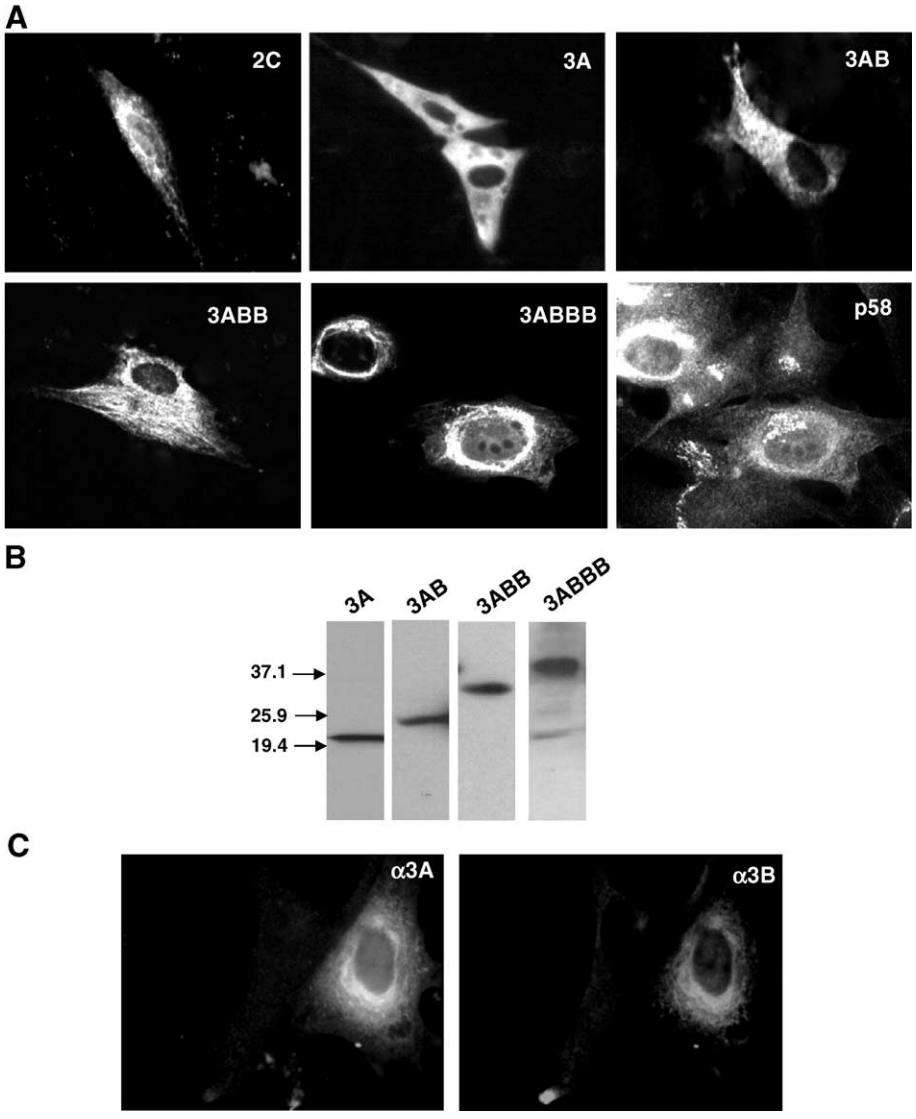

Fig. 4. Transient expression of different FMDV NSPs. BHK-21 cells were transfected with plasmids expressing the proteins indicated, as described in Materials and methods. Results correspond to 24 h p.t. In both immunofluorescence staining (A) or Western blotting (B), 2C expression was detected with MAb 1C8 and MAb 2C2 was used to evaluate the expression of 3A, 3AB, 3ABB and 3ABBB proteins. (C) Expression of 3A or 3B detected, in cells transfected with pRSV-3ABBB, by using rabbit antiserum E12 and MAb 1F8, respectively.

pattern (Fig. 4A). This distribution was maintained when an MAb to 3B (1F8) was used in the immunofluorescence assays (Fig. 4C). In this case, double immunofluorescence studies showed a partial co-localization of 3ABBB with p58 K (Fig. 4A) and no overlap with PDI (data not shown). When 3ABBB was detected in transfected cell extracts, a minor additional band corresponding to mature 3A was also observed (Fig. 4B), supporting a limited proteolytic processing of 3ABBB. The identity of this 3A band was confirmed as it was not recognized by MAb 1F8 to 3B. Processed 3A could also be observed in Western blots from cells transiently expressing 3ABB and 3AB, and the intensity of the band corresponding to mature 3A varied between experiments (data not shown). Further experiments, including other cell lines, are in progress to characterize this processing, which suggests that cellular proteases can cleave the 3B copies included in these precursors.

Transient expression of FMDV 3C was reported as toxic for BHK-21 cells (Martinez-Salas and Domingo, 1995), resulting in a very low number of viable cells; therefore, this protein was not included in our analysis.

Cells transfected with pRSV-3D showed a higher expression efficiency of about 30%. Fluorescence to $3D^{pol}$ was also more intense than that observed for the other FMDV polypeptides analyzed (Fig. 5A). Interestingly, $3D^{pol}$ staining was present all over the cytoplasm and in the nucleus. In these experiments, when double labeling to PDI and $3D^{pol}$ was performed, alterations in the ER could be observed in most of the $3D^{pol}$ expressing cells. Some transfected cells exhibited a more compact and bright ER fluorescence (Fig. 5A, a, c), whereas in cells exhibiting a more intense $3D^{pol}$ nuclear staining, a diffuse ER was frequently observed, including cells in which PDI staining was not detected (Fig. 5A, b, d). This result suggests

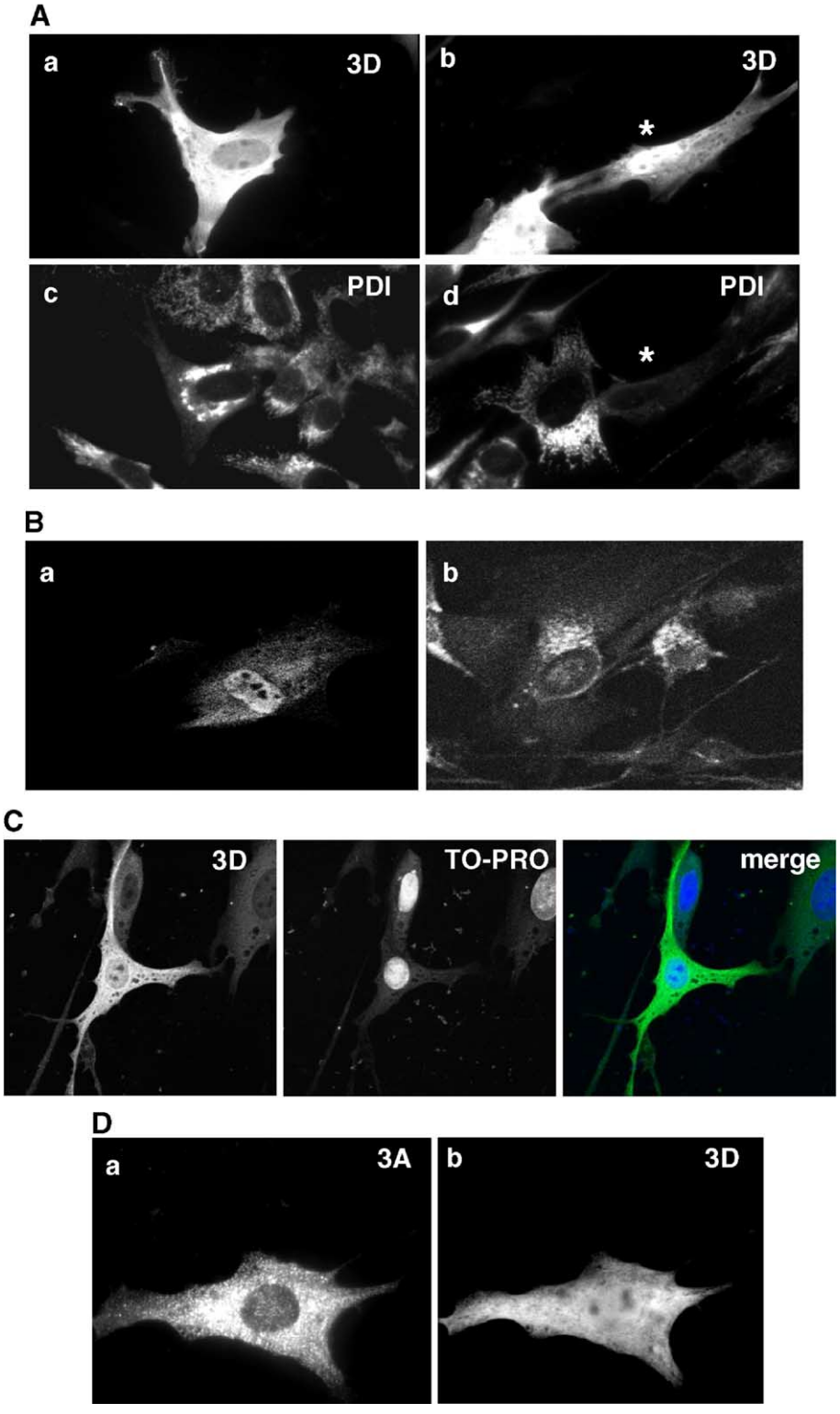

Fig. 5. Effects of expression of 3D in transfected and infected BHK-21 cells. (A) Double immunofluorescence to $3D^{pol}$ (E56) (a, b) and PDI (1D3) (c, d) in cells transfected with pRSV-3D; (*) denotes a cell with a high level of nuclear expression that showed a decrease in ER staining. (B) Immunostaining to 3D in confocal sections of cells transfected with pRSV-3D (a) or after 3.5 h of infection with FMDV (b). (C) Fluorescence to $3D^{pol}$, nuclear staining with TO-PRO-3 and the merge image in cells transfected with p-RSV-3D. (D) Immunostaining to 3A and 3D in cells co-transfected with plasmids pRSV-3ABBB and pRSV-3D. Transfected cells were analyzed, in all cases, at 24 h p.t. Expression of $3D^{pol}$ and 3A was detected with rabbit serum E56 and MAb 2C2, respectively. In all cases, Alexa Fluor 488 anti-rabbit and Alexa Fluor 594 anti-mouse IgGs were used as secondary antibodies.

that ER disruption or rearrangements can take place in $3D^{pol}$ expressing cells.

Nuclear localization of $3D^{pol}$ was supported by confocal microscopy of BHK-21 cells transfected with pRSV-3D, in which this protein was detected in cell nucleus sections (Fig. 5B, a) and its fluorescence co-localized with that of a double-stranded nucleic acid stain (TO-PRO-3) (Fig. 5C). Interestingly, a similar analysis also showed the presence of $3D^{pol}$ in the nucleus of infected cells, albeit the levels of nuclear fluorescence detected were lower than those of transfected cells (Fig. 5B, b). Furthermore, both the cytoplasmic and the nuclear fractions from either FMDV-infected or pRSV-3D transfected BHK-21 cells contained $3D^{pol}$, as estimated by a Western blot assay of these fractions using E56 serum to this protein (Fig. 6). The specificity of this cell fractionation was supported by the low amount of βII-tubulin detected in the nuclear fractions, which could be due to the dragging of the centrosome during sedimentation. In this assay, an additional band corresponding to the expected size for precursor $3CD^{pol}$ (75.7 kDa) was detected in the nuclear fraction of infected cells (Fig. 6B). The specificity of this band was confirmed as it was also detected by MAb 2D2 to 3C (data not shown).

As mentioned in Introduction, interactions between 3AB and $3D^{pol}$ have been reported for poliovirus. Thus, we explored whether the 3ABBB fibrous pattern was maintained when co-expressed with $3D^{pol}$. To this end, plasmids pRSV-3D and pRSV-3ABBB were used in co-transfection experiments for further immunofluorescence analysis using specific antibodies. Under these conditions, the pattern showed by $3D^{pol}$ was similar to that observed when individually expressed, while a noticeable change was observed for 3ABBB, which shifted from the fibrous and perinuclear pattern shown when expressed

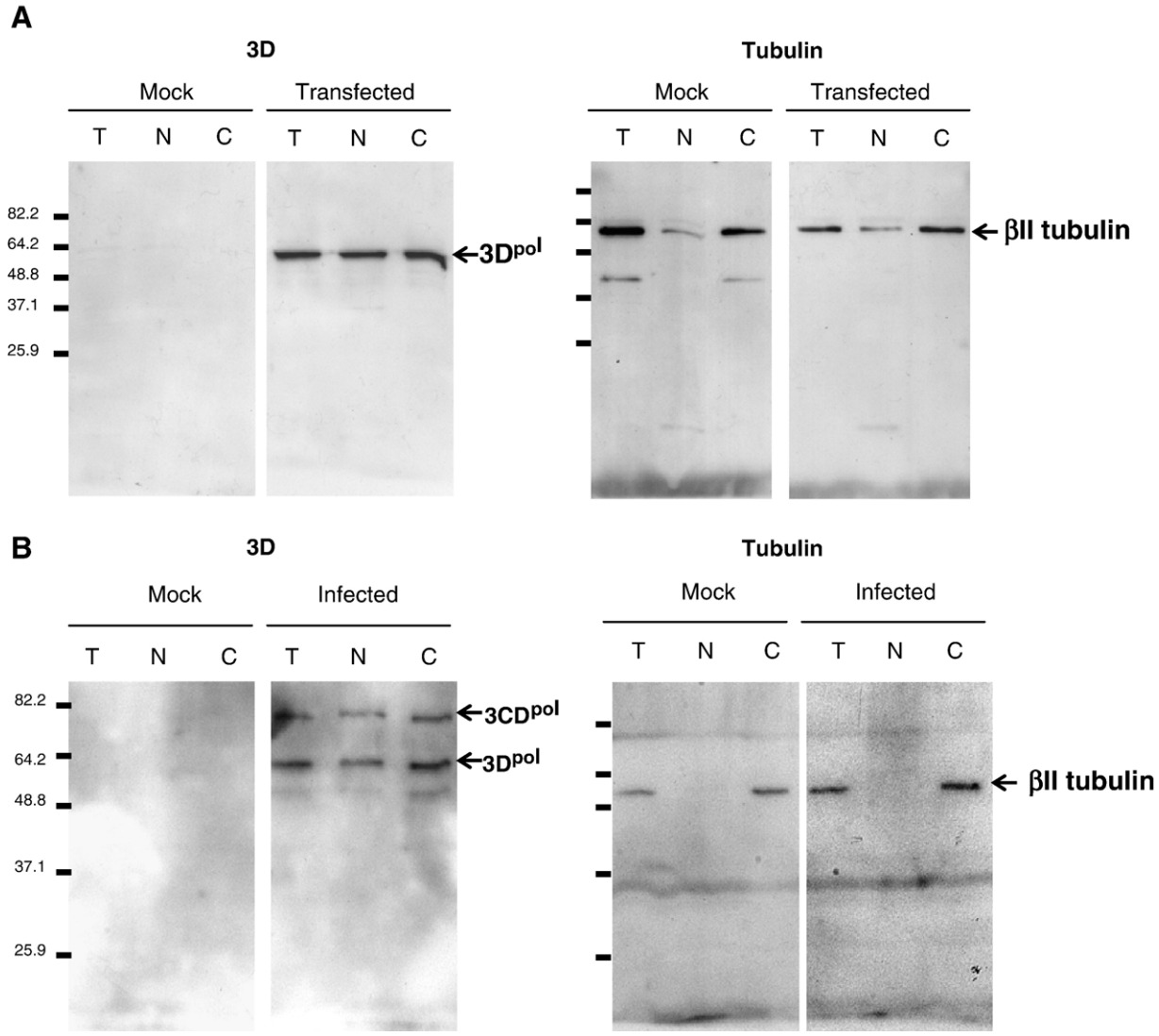

Fig. 6. Western blot analysis of cellular fractions. BHK-21 cells were either infected with C-S8c1 FMDV (A) or transfected with pRSV-3D (B). At 4 h p.i. or 24 h p.t., total cell extracts (T), cytoplasmic and cell membrane fraction (C) and nuclear fraction (N) were obtained (as described in Materials and methods) and assayed by Western blotting using the following antibodies to: 3D (E56) and βII-tubilin (cytoplasmic marker). The migration of the markers and their molecular weight are indicated. Arrows point to the bands corresponding to $3D^{pol}$, $3CD^{pol}$ and βII-tubilin (50 kDa).

alone (see Fig. 4A), to a spotted pattern (Fig. 5D, a). Thus, when co-expressed, $3D^{pol}$ modifies the cellular distribution of 3ABBB.

Discussion

The analysis by immunofluorescence of the kinetics of expression and cell distribution of type C FMDV NSPs in infected cells indicates that, from 3 h p.i., fluorescence to 2B, 2C, 3A, 3B, 3C and $3D^{pol}$, as well as to capsid protein VP1, appeared accumulated at one side of the nucleus, as reported for serotype O viruses (Knox et al., 2005; Monaghan et al., 2004; O'Donnell et al., 2001). This location pattern has been associated to the viral replication complex (Monaghan et al., 2004) as it is well established in other Picornaviruses such as poliovirus (Bienz et al., 1992). However, the partial co-localization of 2C and 3A observed at 3.5 h p.i. suggests that these NSPs can interact with different cell components at advanced stages of FMDV infection.

Detection of FMDV proteins by Western blotting during infection was delayed in time compared to that achieved by immunofluorescence, probably reflecting the asynchrony in the infection progress shown by individual cells and/or a lower sensitivity in this technique of the antibodies used. The earliest protein detected (2.5 h p.i.) was 2C, followed by 2BC, 3ABBB, P1 and VP1 at 3.5 h p.i. From 4 h p.i., all mature proteins analyzed were detected, as well as precursors 2BC, 3AB and 3CD (Fig. 1A).

The origin of the membranes generated at FMDV replication site is unclear (Knox et al., 2005). By electron microscopy, type O FMDV-infected BHK-38 cells showed independent virus-induced vesicles with a low proportion of double membranes (Monaghan et al., 2004), similar to those observed in type C FMDV-infected BHK-21 cells (García-Briones, unpublished results). Previous analyses of FMDV NSPs distribution by immunofluorescence focused on times beyond 3 h p.i., an infection stage in which cells have already developed clear morphological alterations (Monaghan et al., 2004). Protein 3A was reported to co-localize by conventional fluorescence microscopy with the ER marker calreticulin in bovine and porcine keratinocytes ex-vivo-infected with a type O virus (O'Donnell et al., 2001). At the other hand, no co-localization was found in confocal microscopy studies between 2C and markers from ER (ERp57 and ERGIC53) and Golgi (ManII) in CHO-K1 cells or markers of post-Golgi membranes in GMK cells, both infected with a different type O FMDV strain (Knox et al., 2005). Our results indicate that, as described by O'Donnell et al. (2001), 3A co-localizes by confocal microscopy with calreticulin but not with calnexin, while co-localization of 2C with these ER markers was not observed (Figs. 3A, B). On the other hand, 3A and 2C partially co-localize with the Golgi stacks marker p58, but not with the *cis*-Golgi network protein gp74 (Figs. 3C, D). Our observations, which could be related to the cell line used, suggest that, at advanced stages of infection, FMDV NSPs can associate to markers from different membrane compartments.

Interestingly, our results also suggest that NSPs can interact with different cell components during the early steps of FMDV infection. This is probably required to take control of cell machinery and to recruit the cellular factors needed for the formation of the replication complex as it is observed at later stages of infection. Differences have been found in the kinetics and distribution of NSPs fluorescence in infected cells at early times post-infection (1.5–2.5 h p.i.). Specific $3D^{pol}$ immunostaining was detected as soon as 1.5 h pi, while the rest of NSPs and VP1 were detected only from 2 to 2.5 h p.i. (Fig. 2). This delay can be due to a higher sensitivity of the $3D^{pol}$ antiserum used, although differences such us protein accessibility and/or different local concentration cannot be excluded. At these early times of infection, VP1, 2B, 2C and 3C mostly exhibited a punctuated and scattered pattern, while immunostaining to 3A showed a perinuclear distribution similar to that of $3D^{pol}$ (2 h p.i.), which suggests that early interactions can be established between these two proteins.

Transient expression analyses in BHK-21 cells have revealed differences in the cellular distribution of some of the FMDV NSPs studied. The lack of detection of 2B upon transfection with pRSV-2B is likely to result from low levels of protein expression, probably due to cell toxicity. Thus, detection of 2B transient expression has been reported by using a modified 2B, including a tag motif (Moffat et al., 2005). Besides, the low levels of expression and the elongated morphology of cells transfected with 2C also suggest a detrimental effect of its expression on cell viability. In this case, the subcellular distribution observed for 2C (Fig. 4A) was similar to that displayed at early times post-infection (Fig. 2).

Higher levels of expression were detected by using an MAb to 3A in cells transfected with plasmids corresponding to the different products of the 3ABBB region. Expression of 3A resulted in a diffused and spotted pattern, similar to that shown by cells soon after infection (Fig. 2), which suggested the localization of 3A at small vesicles, as it has been reported for FMDV type O in BHK-21 and other cultured cells (Moffat et al., 2005; O'Donnell et al., 2001). No previous information was available, to our knowledge, on the cellular distribution of the remaining products from the FMDV 3AB region. Remarkably, our results indicate that sequential addition of protein B copies resulted in a relocation of 3A fluorescence that became progressively compact and fibrous. A typical vesicular pattern was clearly observed upon 3AB transfection, indicating that 3AB can become associated to cell vesicles. 3AB is the most abundant 3B-containing precursor in FMDV-infected cells (Fig. 1A) even at late times post-infection, as also found for type A and type O FMDV-infected cells (O'Donnell et al., 2001). This vesicular pattern shifted to a fibrous network in cells expressing 3ABB, being the change most evident in 3ABBB expressing cells (Fig. 4A), which exhibited a fibrous perinuclear distribution when visualized with antibodies to either 3A or 3B (Fig. 4C). The interactions leading to these different distributions remain to be determined. Experiments are in progress to analyze the cell distribution of transiently expressed 3B products as well as their effect in co-expression experiments with 3A. Double staining with Golgi p58 or PDI only revealed a partial co-localization of 3ABBB with the Golgi stacks; however, this co-localization was not observed for 3A and 3AB. In poliovirus,

expression of 3A alone inhibits ER to Golgi protein traffic (Doedens and Kirkegaard, 1995) and dramatically alters the ER structure (Doedens et al., 1997), an effect not observed when 3AB is expressed alone (Egger et al., 2000).

Cells transfected with $3D^{pol}$ showed the highest level of expression of all NSPs. $3D^{pol}$ was homogeneously distributed in the cell, including the nucleus, and induced partial reorganization of the ER, as estimated by the use of an anti-PDI antibody. A confocal analysis confirmed the nuclear localization of $3D^{pol}$ in transfected cells (Figs. 5B, C). This observation led us to perform a similar analysis in FMDV-infected cells that showed $3D^{pol}$ nuclear staining in the sections analyzed (Fig. 5B). The presence of $3D^{pol}$ in the nucleus was confirmed by its detection in the nuclear fraction of transfected and infected cells (Fig. 6). Ultrastructural modifications of the nuclear membrane have been recently described in FMDV-infected cells (Monaghan et al., 2004). Furthermore, nuclear location of NSPs, including precursors containing $3D^{pol}$, has been recently reported for rhinovirus and encephalmyocartitis virus, suggesting that Picornaviruses can reprogram the cell nucleus as part of their replication cycle (Aminev et al., 2003; Amineva et al., 2004). These authors also identified a nuclear localization motif (PnKTKLnPS) near the N-terminus of $3D^{pol}$. A similar sequence (MRKTKLnPT) is present at equivalent positions of FMDV $3D^{pol}$ sequences (residues 16–24) among a wide variety of FMDV isolates representing the seven serotypes (Carrillo et al., 2005), including the C-S8c1 isolate used in this study. In FMDV, histone H3 can be in vitro cleavage by 3C (Falk et al., 1990), a processing also reported in BHK-21 cells transiently expressing 3C (Tesar and Marquardt, 1990) and 3ABC (Capozzo et al., 2002). Our results indicate that a protein band corresponding to $3CD^{pol}$ is also present, with a weaker intensity than that of $3D^{pol}$, in nuclear fractions of infected cells (Fig. 6). Translocation of $3CD^{pol}$ to the nucleus might favor and/or modulate 3C nuclear activity in FMDV-infected cells. To our knowledge, these results are the first evidences of nuclear localization of FMDV proteins and experiments are in progress to understand their functional implications in FMDV replication.

Co-expression with $3D^{pol}$ modified the distribution of 3ABBB that shifts to a pattern similar to that observed in cells expressing 3AB (Fig. 5D). Interactions between 3A and $3D^{pol}$ are suggested by their common fluorescence pattern observed early upon infection (Fig. 2). However, further work is required to establish the protein regions involved in this relocation of 3ABBB and whether it is mediated by an interaction with $3D^{pol}$, as that reported in poliovirus (Lama et al., 1994; Xiang et al., 1995) or by cell modifications induced by this protein in transfected cells.

Materials and methods

Cells and viruses

BHK-21 cells (ATCC) were maintained in Dulbecco's modified Eagle's medium (DMEM) (Gibco-BRL) supplemented with 5% fetal bovine serum (Gibco-BRL), 2 mM L-glutamine, 1 μg/ml streptomycin and 1 μg/ml penicillin. Cells from passages 10–20 were infected with the type C FMDV isolate, C-S8c1 (Sobrino et al., 1986).

Construction of plasmids

Plasmids for transient expression were derived from plasmid pRSV/L (de Wet et al., 1987) in which the luciferase gene was replaced by each of the following NSPs coding sequences: 2B, 2C, 3A, 3AB, 3ABB, 3ABBB and $3D^{pol}$. Each of these sequences was amplified by PCR from either FMDV C-S8c1 RNA or plasmid MT15 (Toja et al., 1999), using the primers detailed in Table 1, which included restriction sites for cloning into plasmid pRSV/L. Integrity of all PCR-amplified regions within the recombinant vectors was confirmed by nucleotide sequencing.

Virus infections and cell transfections

BHK-21 confluent cells were infected with a multiplicity of infection (m.o.i) of 10 PFU/cell. After 1 h of virus adsorption, which was considered as 1 h post-infection (p.i.), cells were washed and the infection allowed proceeding in fresh medium. Subconfluent monolayers of cells grown on 10 mm Ø glass

Table 1
Oligonucleotides used for PCR amplification of NSPs sequences

Oligonucleotide[a]	Sequence (5′-3′)[b]
2B-1	ATACCCGGGTCTAGAA*TG*CCCTTCTTCTTCTCT *Sma*I 2B
2B-2	GCGGTACCCCATGGTCTAGA**TTA**TTGTTTCTCTGCTCT *Kpn*I 2B
2C-1	TCTAGAAAGCTTA*TG*CTCAAAGACCGTGAC *Hind*III 2C
2C-2	TCTAGAGGTACC**TTA**TTGCTTAAAAATTGG *Kpn*I 2C
3A-1	GCGAAGCTTTCTAGAA*TG*ATCTCAATACCTTCC *Hind*III 3A
3A-2	TATAGTTCTGGTACC**TTA**TTCAGCTTGCGGTTG *Kpn*I 3A
3AB-2	AGGTACCCCATGGTCTAGA**TTA**CTCTTGTCGCGGGAG *Kpn*I 3B
3ABB-2	TAGGTACC**TTA**TTCCTTGACGACCGGGGC *Kpn*I 3B
3ABBB-2	TCTAGAGGTACC**TTA**CTCAGTGACAATCAA *Kpn*I 3B
3D-1	CGCCCGGG*ATG*GGGTTGATCGTTGAT *Sma*I 3D
3D-2	CAGGTACC**TTA**TGCGTCGCCGCACACG *Kpn*I 3D

[a] Forward and reverse primers are indicated by -1 and -2, respectively.
[b] Restriction sites introduced for cloning into pRSV vector are indicated and their nucleotides underlined. AUG initiator is shown in italics. UAA stop codon is shown in bold. The specific nucleotides for each NSPs are underlined.

coverslips in 24-well tissue culture dishes were transfected with 0.25 μg of each of the different pRSV derivatives, using Lipofectamine Plus reagent (Gibco-BRL).

Antibodies and stains

Rabbit polyclonal sera against the following FMDV proteins were used: 2B (DM21) kindly provided by D. Mackay (Institute of Animal Health of Pirbright, UK), 2C (E39), 3A (E12) and $3D^{pol}$ (E56) (Strebel et al., 1986). In addition, MAbs to 2C (1C8), 3A (2C2), 3B (1F8) and 3C (2D2), kindly provided by E. Brocchi (Istituto Zooprofilattico Sperimentale della Lombardia e dell'Emilia-Romagna, Brescia, Italy) and to VP1 (SD6) (Mateu et al., 1987), were employed. The following antibodies to cell proteins were employed: MAb anti-Golgi stacks protein p58 (Sigma), MAb 1D3 against PDI (protein disulfide isomerase) and rabbit serum anti-calnexin (ER markers, obtained from Stressgene), MAb CC92 to the *cis*-Golgi network protein gp74 (Alcalde et al., 1994), as well as rabbit sera to human calreticulin (Abcam) and βII-tubulin (Armas-Portela et al., 1999). Horseradish-peroxidase (HRP)-coupled anti-mouse or anti-rabbit antibodies were from Amersham. Goat antibodies anti-mouse and anti-rabbit IgGs coupled to Alexa 594 or 488 were from Molecular Probes. TO-PRO-3 double-stranded nucleic acid stain (Molecular Probes) was used for nuclear staining.

Western blot analysis

BHK-21 cell monolayers either FMDV-infected or transfected with different plasmids as described above were collected from cultured dishes (35 mm Ø) in lysis buffer (10 mM EGTA, 2.5 mM $MgCl_2$, 1% NP-40 and 20 mM HEPES, pH 7.4) supplemented with a 1 mM PMSF and protease inhibitor cocktail (Roche). After 10 min sonication, samples were boiled for 4 min in Laemmli buffer and resolved on a 12% SDS-PAGE. Proteins were transferred onto a nitrocellulose membrane and incubated with specific FMDV antibodies, then with HRP-coupled anti-mouse or anti-rabbit antibodies and subsequently developed using an ECL kit (Amersham).

Cellular fractionation

Monolayers of BHK-21 cells (grown in 60 mm Ø dishes), either FMDV-infected or transfected with plasmids, were washed with PBS, detached from plates by scrapping, collected by centrifugation at 110 × *g* for 5 min and resuspended in 0.25 M sucrose in buffer A (50 mM Tris, 5 mM EDTA, 1 mM $MgCl_2$, 0.5% Triton X-100), supplemented with 1 mM PMSF and protease inhibitor cocktail. Suspensions were homogenized in ice by needle (20-gauge) passage and sonication (total homogenate). Nuclei were separated from cytoplasmic and membrane components (cytoplasmic fraction) by centrifugation at 440 × *g* for 20 min at 4 °C. The resulting pellet (nuclear fraction) was washed three times with sucrose buffered and resuspended in buffer A. Protein concentration was determined by Bradford, and equal amounts from each fraction, in Laemmli buffer, were analyzed by SDS-polyacrylamide gel electrophoresis, as described above.

Immunofluorescence assays

Cells cultured on coverslips were infected or transfected as detailed above. At different times p.i., or 24 h post-transfection (p.t.), cells were fixed with 4% paraformaldehyde for 20 min, blocked and permeabilized by incubating in PBTG buffer (0.1% Triton X-100; 1% bovine serum albumin; 1 M glycine in phosphate-buffered saline, PBS) for 15 min at room temperature. Subsequently, cells were incubated with primary antibodies for 1 h, washed in PBS, incubated with fluorescent-labeled secondary antibodies for 30 min and mounted in Fluoromount-G (Southern Biotech. Assoc., USA). Nuclear staining with TO-PRO-3 was performed as recommended by the manufacturers.

Microscopy and confocal analyses

Cell preparations were viewed with an Olympus BX61 or a Confocal Radiance-2000 (BioRad/Zeiss) microscope. Images were processed with Adobe Photoshop software. Co-localization analyses after confocal images were realized using the Metamorph offline software.

Acknowledgments

We wish to thank E. Beck, E. Brocchi and D. McKay for providing us with antibodies to FMDV NSPs. We also thank C. Aparicio for her contribution to pRSV-3ABB construction, I. Sandoval, I. Correas and L. Kremer for providing us with antibodies to cell proteins and M. Saiz for her critical review of the manuscript. This work was supported by grants from CICYT, Spain (BIO2005-07592-C02-01), EU (QLK2-2001-1304) and by Fundación Severo Ochoa.

References

Alcalde, J., Egea, G., Sandoval, I.V., 1994. gp74 a membrane glycoprotein of the *cis*-Golgi network that cycles through the endoplasmic reticulum and intermediate compartment. J. Cell Biol. 124 (5), 649–665.

Aldabe, R., Carrasco, L., 1995. Induction of membrane proliferation by poliovirus proteins 2C and 2BC. Biochem. Biophys. Res. Commun. 206 (1), 64–76.

Aminev, A.G., Amineva, S.P., Palmenberg, A.C., 2003. Encephalomyocarditis virus (EMCV) proteins 2A and 3BCD localize to nuclei and inhibit cellular mRNA transcription but not rRNA transcription. Virus Res. 95 (1–2), 59–73.

Amineva, S.P., Aminev, A.G., Palmenberg, A.C., Gern, J.E., 2004. Rhinovirus 3C protease precursors 3CD and 3CD′ localize to the nuclei of infected cells. J. Gen. Virol. 85 (Pt. 10), 2969–2979.

Andino, R., Boddeker, N., Silvera, D., Gamarnik, A.V., 1999. Intracellular determinants of picornavirus replication. Trends Microbiol. 7 (2), 76–82.

Arlinghaus, R.B., Polatnick, J., 1969. The isolation of two enzyme–ribonucleic acid complexes involved in the synthesis of foot-and-mouth disease virus ribonucleic acid. Proc. Natl. Acad. Sci. U.S.A. 62 (3), 821–828.

Armas-Portela, R., Parrales, M.A., Albar, J.P., Martinez, A.C., Avila, J., 1999. Distribution and characteristics of betaII tubulin-enriched microtubules in interphase cells. Exp. Cell Res. 248 (2), 372–380.

Bachrach, H.L., 1977. Foot-and-mouth disease virus, properties, molecular biology and immunogenicity. In: Romberger, J.A. (Ed.), Beltsville Symposia in Agricultural Research. Virology in Agriculture, vol. 1. Allanheld, Osmun & Co., Montclair, NJ.

Barteling, S.J., 2004. Modern inactivated Foot-and-mouth disease (FMD) vaccines: historical background and key elements in production and use. In: Domingo, F.S.a.E. (Ed.), Foot-and-Mouth Disease: Current Perspectives. Horizon Bioscience, Norfolk.

Beard, C.W., Mason, P.W., 2000. Genetic determinants of altered virulence of Taiwanese foot-and-mouth disease virus. J. Virol. 74 (2), 987–991.

Beck, E., Forss, S., Strebel, K., Cattaneo, R., Feil, G., 1983. Structure of the FMDV translation initiation site and of the structural proteins. Nucleic Acids Res. 11 (22), 7873–7885.

Belsham, G.J., 2005. Translation and replication of FMDV RNA. Curr. Top. Microbiol. Immunol. 288, 43–70.

Belsham, G.J.a.M.-S., E., 2004. Genome organization, translation and replication of foot-and-mouth disease virus. In: Domingo, F.S.A.E. (Ed.), Foot-and-mouth Disease. Current Perspectives. Horizon Bioscience, Norfolk, UK, pp. 19–52.

Bienz, K., Egger, D., Pasamontes, L., 1987. Association of polioviral proteins of the P2 genomic region with the viral replication complex and virus-induced membrane synthesis as visualized by electron microscopic immunocytochemistry and autoradiography. Virology 160 (1), 220–226.

Bienz, K., Egger, D., Pfister, T., Troxler, M., 1992. Structural and functional characterization of the poliovirus replication complex. J. Virol. 66 (5), 2740–2747.

Bolten, R., Egger, D., Gosert, R., Schaub, G., Landmann, L., Bienz, K., 1998. Intracellular localization of poliovirus plus- and minus-strand RNA visualized by strand-specific fluorescent in situ hybridization. J. Virol. 72 (11), 8578–8585.

Brown, F., 1998. Problems with BHK 21 cells. Dev. Biol. Stand. 93, 85–88.

Burrows, R., Mann, J.A., Garland, A.J., Greig, A., Goodridge, D., 1981. The pathogenesis of natural and simulated natural foot-and-mouth disease infection in cattle. J. Comp. Pathol. 91 (4), 599–609.

Capozzo, A.V., Burke, D.J., Fox, J.W., Bergmann, I.E., La Torre, J.L., Grigera, P.R., 2002. Expression of foot and mouth disease virus non-structural polypeptide 3ABC induces histone H3 cleavage in BHK21 cells. Virus Res. 90 (1–2), 91–99.

Carrillo, C., Tulman, E.R., Delhon, G., Lu, Z., Carreno, A., Vagnozzi, A., Kutish, G.F., Rock, D.L., 2005. Comparative genomics of foot-and-mouth disease virus. J. Virol. 79 (10), 6487–6504.

Cho, M.W., Teterina, N., Egger, D., Bienz, K., Ehrenfeld, E., 1994. Membrane rearrangement and vesicle induction by recombinant poliovirus 2C and 2BC in human cells. Virology 202 (1), 129–145.

Choe, S.S., Dodd, D.A., Kirkegaard, K., 2005. Inhibition of cellular protein secretion by picornaviral 3A proteins. Virology 337 (1), 18–29.

de Wet, J.R., Wood, K.V., DeLuca, M., Helinski, D.R., Subramani, S., 1987. Firefly luciferase gene: structure and expression in mammalian cells. Mol. Cell. Biol. 7 (2), 725–737.

Deitz, S.B., Dodd, D.A., Cooper, S., Parham, P., Kirkegaard, K., 2000. MHC I-dependent antigen presentation is inhibited by poliovirus protein 3A. Proc. Natl. Acad. Sci. U.S.A. 97 (25), 13790–13795.

Doedens, J.R., Kirkegaard, K., 1995. Inhibition of cellular protein secretion by poliovirus proteins 2B and 3A. EMBO J. 14 (5), 894–907.

Doedens, J.R., Giddings Jr., T.H., Kirkegaard, K., 1997. Inhibition of endoplasmic reticulum-to-Golgi traffic by poliovirus protein 3A: genetic and ultrastructural analysis. J. Virol. 71 (12), 9054–9064.

Domingo, E., Mateu, M.G., Martínez, M.A., Dopazo, J., Moya, A., Sobrino, F., 1990. Genetic variability and antigenic diversity of foot-and-mouth disease virus. In: Kurstak, R.G.M.E., Murphy, S.A., Van-Regenmortel, M.H.V. (Eds.), Applied Virology Research. Virus Variation and Epidemiolgy, vol. 2. Academic Press Inc., London.

Egger, D., Teterina, N., Ehrenfeld, E., Bienz, K., 2000. Formation of the poliovirus replication complex requires coupled viral translation, vesicle production, and viral RNA synthesis. J. Virol. 74 (14), 6570–6580.

Falk, M.M., Grigera, P.R., Bergmann, I.E., Zibert, A., Multhaup, G., Beck, E., 1990. Foot-and-mouth disease virus protease 3C induces specific proteolytic cleavage of host cell histone H3. J. Virol. 64 (2), 748–756.

Falk, M.M., Sobrino, F., Beck, E., 1992. VPg gene amplification correlates with infective particle formation in foot-and-mouth disease virus. J. Virol. 66 (4), 2251–2260.

Follett, E.A., Pringle, C.R., Pennington, T.H., 1975. Virus development in enucleate cells: echovirus, poliovirus, pseudorabies virus, reovirus, respiratory syncytial virus and Semliki Forest virus. J. Gen. Virol. 26 (2), 183–196.

Forss, S., Strebel, K., Beck, E., Schaller, H., 1984. Nucleotide sequence and genome organization of foot-and-mouth disease virus. Nucleic Acids Res. 12 (16), 6587–6601.

Gazina, E.V., Mackenzie, J.M., Gorrell, R.J., Anderson, D.A., 2002. Differential requirements for COPI coats in formation of replication complexes among three genera of Picornaviridae. J. Virol. 76 (21), 11113–11122.

Gosert, R., Egger, D., Bienz, K., 2000. A cytopathic and a cell culture adapted hepatitis A virus strain differ in cell killing but not in intracellular membrane rearrangements. Virology 266 (1), 157–169.

Hope, D.A., Diamond, S.E., Kirkegaard, K., 1997. Genetic dissection of interaction between poliovirus 3D polymerase and viral protein 3AB. J. Virol. 71 (12), 9490–9498.

Jackson, C.L., Casanova, J.E., 2000. Turning on ARF: the Sec7 family of guanine–nucleotide-exchange factors. Trends Cell Biol. 10 (2), 60–67.

Klausner, R.D., Donaldson, J.G., Lippincott-Schwartz, J., 1992. Brefeldin A: insights into the control of membrane traffic and organelle structure. J. Cell Biol. 116 (5), 1071–1080.

Knox, C., Moffat, K., Ali, S., Ryan, M., Wileman, T., 2005. Foot-and-mouth disease virus replication sites form next to the nucleus and close to the Golgi apparatus, but exclude marker proteins associated with host membrane compartments. J. Gen. Virol. 86 (Pt. 3), 687–696.

Lama, J., Paul, A.V., Harris, K.S., Wimmer, E., 1994. Properties of purified recombinant poliovirus protein 3aB as substrate for viral proteinases and as co-factor for RNA polymerase 3Dpol. J. Biol. Chem. 269 (1), 66–70.

Martinez-Salas, E., 1999. Internal ribosome entry site biology and its use in expression vectors. Curr. Opin. Biotechnol. 10 (5), 458–464.

Martinez-Salas, E., Domingo, E., 1995. Effect of expression of the aphthovirus protease 3C on viral infection and gene expression. Virology 212 (1), 111–120.

Mateu, M.G., Rocha, E., Vicente, O., Vayreda, F., Navalpotro, C., Andreu, D., Pedroso, E., Giralt, E., Enjuanes, L., Domingo, E., 1987. Reactivity with monoclonal antibodies of viruses from an episode of foot-and-mouth disease. Virus Res. 8 (3), 261–274.

Moffat, K., Howell, G., Knox, C., Belsham, G.J., Monaghan, P., Ryan, M.D., Wileman, T., 2005. Effects of foot-and-mouth disease virus nonstructural proteins on the structure and function of the early secretory pathway: 2BC but not 3A blocks endoplasmic reticulum-to-Golgi transport. J. Virol. 79 (7), 4382–4395.

Monaghan, P., Cook, H., Jackson, T., Ryan, M., Wileman, T., 2004. The ultrastructure of the developing replication site in foot-and-mouth disease virus-infected BHK-38 cells. J. Gen. Virol. 85 (Pt. 4), 933–946.

Nayak, A., Goodfellow, I.G., Belsham, G.J., 2005. Factors required for the uridylylation of the foot-and-mouth disease virus 3B1, 3B2, and 3B3 peptides by the RNA-dependent RNA polymerase (3Dpol) in vitro. J. Virol. 79 (12), 7698–7706.

Newman, J.F., Cartwright, B., Doel, T.R., Brown, F., 1979. Purification and identification of the RNA-dependent RNA polymerase of foot-and-mouth disease virus. J. Gen. Virol. 45 (2), 497–507.

Nunez, J.I., Baranowski, E., Molina, N., Ruiz-Jarabo, C.M., Sanchez, C., Domingo, E., Sobrino, F., 2001. A single amino acid substitution in nonstructural protein 3A can mediate adaptation of foot-and-mouth disease virus to the guinea pig. J. Virol. 75 (8), 3977–3983.

O'Donnell, V.K., Pacheco, J.M., Henry, T.M., Mason, P.W., 2001. Subcellular distribution of the foot-and-mouth disease virus 3A protein in cells infected with viruses encoding wild-type and bovine-attenuated forms of 3A. Virology 287 (1), 151–162.

Pacheco, J.M., Henry, T.M., O'Donnell, V.K., Gregory, J.B., Mason, P.W., 2003. Role of nonstructural proteins 3A and 3B in host range and pathogenicity of foot-and-mouth disease virus. J. Virol. 77 (24), 13017–13027.

Pereira, H.G., 1981. Foot-and-mouth disease. In: Gibbs, E.P.J. (Ed.), Virus Disease of Food Animals, vol. 2. Academic Press Inc, London.

Porter, A.G., 1993. Picornavirus nonstructural proteins: emerging roles in virus replication and inhibition of host cell functions. J. Virol. 67 (12), 6917–6921.

Ryan, M.D., Donelly, M.L.L., Flint, M., Cowton, V.M., Luke, G., Hughes, L.E., Knox, C., de Felipe, P., 2004. Foot-and-mouth disease proteinases. In: Domingo, F.S.a.E. (Ed.), Foot-and-Mouth Disease. Current Perspectives. Horizon Bioscience, Norfolk, UK, pp. 53–76.

Sandoval, I.V., Carrasco, L., 1997. Poliovirus infection and expression of the poliovirus protein 2B provoke the disassembly of the Golgi complex, the organelle target for the antipoliovirus drug Ro-090179. J. Virol. 71 (6), 4679–4693.

Sanz-Parra, A., Sobrino, F., Ley, V., 1998. Infection with foot-and-mouth disease virus results in a rapid reduction of MHC class I surface expression. J. Gen. Virol. 79 (Pt. 3), 433–436.

Schlegel, A., Giddings Jr., T.H., Ladinsky, M.S., Kirkegaard, K., 1996. Cellular origin and ultrastructure of membranes induced during poliovirus infection. J. Virol. 70 (10), 6576–6588.

Sobrino, F., Palma, E.L., Beck, E., Davila, M., de la Torre, J.C., Negro, P., Villanueva, N., Ortin, J., Domingo, E., 1986. Fixation of mutations in the viral genome during an outbreak of foot-and-mouth disease: heterogeneity and rate variations. Gene 50 (1–3), 149–159.

Sobrino, F., Saiz, M., Jimenez-Clavero, M.A., Nunez, J.I., Rosas, M.F., Baranowski, E., Ley, V., 2001. Foot-and-mouth disease virus: a long known virus, but a current threat. Vet. Res. 32 (1), 1–30.

Strebel, K., Beck, E., Strohmaier, K., Schaller, H., 1986. Characterization of foot-and-mouth disease virus gene products with antisera against bacterially synthesized fusion proteins. J. Virol. 57 (3), 983–991.

Suhy, D.A., Giddings Jr., T.H., Kirkegaard, K., 2000. Remodeling the endoplasmic reticulum by poliovirus infection and by individual viral proteins: an autophagy-like origin for virus-induced vesicles. J. Virol. 74 (19), 8953–8965.

Tesar, M., Marquardt, O., 1990. Foot-and-mouth disease virus protease 3C inhibits cellular transcription and mediates cleavage of histone H3. Virology 174 (2), 364–374.

Toja, M., Escarmis, C., Domingo, E., 1999. Genomic nucleotide sequence of a foot-and-mouth disease virus clone and its persistent derivatives. Implications for the evolution of viral quasispecies during a persistent infection. Virus Res. 64 (2), 161–171.

Towner, J.S., Ho, T.V., Semler, B.L., 1996. Determinants of membrane association for poliovirus protein 3AB. J. Biol. Chem. 271 (43), 26810–26818.

Whitton, J.L., Cornell, C.T., Feuer, R., 2005. Host and virus determinants of picornavirus pathogenesis and tropism. Nat. Rev., Microbiol. 3 (10), 765–776.

Xiang, W., Harris, K.S., Alexander, L., Wimmer, E., 1995. Interaction between the 5′-terminal cloverleaf and 3AB/3CDpro of poliovirus is essential for RNA replication. J. Virol. 69 (6), 3658–3667.

Xiang, W., Cuconati, A., Hope, D., Kirkegaard, K., Wimmer, E., 1998. Complete protein linkage map of poliovirus P3 proteins: interaction of polymerase 3Dpol with VPg and with genetic variants of 3AB. J. Virol. 72 (8), 6732–6741.